Journal of Molecular Catalysis A: Chemical 420 (2016) 200–207

Contents lists available at ScienceDirect

Journal of Molecular Catalysis A: Chemical

journal homepage: www.elsevier.com/locate/molcata

Sensitization of La modified $NaTaO_3$ with cobalt tetra phenyl porphyrin for photo catalytic reduction of CO_2 by water with UV–visible light

Velu Jeyalakshmi[a,b], Selvaraj Tamilmani[b], Rajaram Mahalakshmy[a], Puttaiah Bhyrappa[c], Konda Ramasamy Krishnamurthy[b], Balasubramanian Viswanathan[b,*]

[a] Department of Chemistry, Thiagarajar College, Madurai Kamaraj University, Madurai-625021, India
[b] National Centre for Catalysis Research, Indian Institute of Technology, Madras, Chennai-600036, India
[c] Department of Chemistry, Indian Institute of Technology, Madras, Chennai-600036, India

ARTICLE INFO

Article history:
Received 5 April 2016
Received in revised form 24 April 2016
Accepted 25 April 2016
Available online 26 April 2016

Keywords:
CO_2 photo reduction
Sodium tantalate
Sensitization
Porphyrins
DFT

ABSTRACT

Lanthanum modified sodium tantalate, $Na_{(1-x)}La_xTaO_{(3+x)}$, in conjunction with cobalt (II) tetra phenyl porphyrin (CoTPP) as sensitizer, has been explored for photo catalytic reduction of carbon dioxide (PCRC) with water. HOMO and LUMO energy level characteristics/redox potentials for ground (S_0) and excited states (S_1 singlet) of CoTPP have been calculated by Density Functional Theory (DFT). HOMO and LUMO energy levels enable sensitization of the tantalate, a typical wide band gap semi-conductor, with visible light. Visible light absorption by CoTPP results in the direct transfer of photo generated electrons to the conduction band of the tantalate, in addition to the intrinsic UV light excitation. Besides, sensitization also retards charge carrier recombination rate, as indicated by the photo luminescence spectral data for the pristine and sensitized $Na_{(1-x)}La_xTaO_{(3+x)}$. A co-operative effect of these factors contributes towards nearly 3 fold increase in apparent quantum yield value for PCRC with the 1% w/w CoTPP/tantalate composite vis-à-vis pristine tantalate. After 20 h of irradiation, rate of methanol formation remains constant with pristine and sensitized tantalates, while the rate of formation of ethanol increases on sensitization, indicating multi electron reduction process. Chemical composition and structural characteristics of the composite are preserved even after 20 h of irradiation.

© 2016 Elsevier B.V. All rights reserved.

1. Introduction

Global demand for energy is set to increase up to 50% by the year 2030. It is expected that fossil fuels would continue to be the major source of energy in the near future. CO_2 emissions from the fossil fuels pose serious environmental issues like green-house gas effect and unusual weather patterns. In this context, conversion of CO_2 into fuels/hydrocarbons is an effective strategy to contain the effects of CO_2 emissions. Photo-catalytic reduction of CO_2 (PCRC) into fuels/hydrocarbons or *artificial photosynthesis*, using water as the reductant, is a complex, challenging and multi-step process with high application potential, to mitigate green house gas effect and project CO_2 as a possible source for sustainable energy. Several investigations focusing on a wide range of heterogeneous photo catalysts for the artificial photo synthesis process have been reported [1–3]. Tantalum based perovskites, in particular, have received considerable attention [4–7] since: (i) the energy of conduction band minimum of tantalum based compounds are more negative compared to other transition metal oxides and also more negative than redox potentials for the conversion of CO_2 to products like CH_3OH, CH_4, C_2H_5OH (ii) tantalates, being ferroelectric materials, have internal dipoles that facilitate separation of electrons and holes, so as to retard recombination rate and increase their life time (iii) bond angle of Ta-O-Ta is close to 180° and hence easy transport of photo electron-hole pairs across the corner-shared octahedral framework is favoured and (iv) alkali metal tantalates are active for chemisorption of CO_2.

Amongst the three alkali metal tantalates, $ATaO_3$ (A = Li, Na & K), $NaTaO_3$ modified with lanthanum and NiO as co-catalyst, displays maximum activity for hydrogen production [8,9] by splitting of water, with a quantum efficiency of 56% under UV radiation (270 nm). Teramura et al. [10] have observed that these alkali metal tantalates catalyse PCRC using external hydrogen as reductant, forming only CO and no hydrocarbons. However, our earlier stud-

* Corresponding author.
E-mail address: bvnathan@iitm.ac.in (B. Viswanathan).

http://dx.doi.org/10.1016/j.molcata.2016.04.027
1381-1169/© 2016 Elsevier B.V. All rights reserved.

ies [11] have shown that La modified $NaTaO_3$, loaded with various co-catalysts, like, Pt, Ag, Au, CuO, NiO and RuO_2, displays significant activity for photo reduction of CO_2, yielding hydrocarbons like methanol, ethanol and methane using water as reductant.

$NaTaO_3$ being a typical wide band gap semi-conductor, absorbs only <5% of solar energy (UV region). Several approaches to improve its visible light activity by doping with cations and anions have been explored [6,12–27]. Sato et al. [28,29] reported CO_2 photo reduction using N-doped Ta_2O_5 linked with Ru complexes, which showed high activity and selectivity towards HCOOH. Sensitization/coupling with light harvesting moieties is yet another strategy for the utilization of visible light by tantalates. Metallo porphyrins are good candidates for such coupling, due to their ability to absorb visible light and their structural similarity with the natural light harvesting moieties [30]. Choice of metal complexes for sensitizing large band gap semiconductor depends on certain characteristics like:

I.) suitable redox potential with respect to the conduction band of the semi-conductor
II.) optical absorption, mainly in the visible solar region,
III.) strongly bound to the semiconductor surface,
IV.) photo conductivity and chemical stability.

Phorphyrin derivatives display the requisite characteristics and have unique values for HOMO and LUMO energy levels to sensitize wide band gap semiconductors like TiO_2 [30]. Porphyrins possess suitable ground and excited state redox potentials with respect to the semiconductor conduction band and a π- electron conjugate system which facilitates conductivity of the material and light absorption in the solar visible region [31–33]. Besides, sensitization results in multi electron reduction products compared to other modifications, due to high conductivity and high absorption co-efficient of such sensitizers within the solar region. Considering such advantages associated with the use of metallo porphyrins, PCRC with water by using Cobalt (II) tetra phenyl porphyrin (CoTPP) as sensitizer for wide band gap photo catalyst $Na_{(1-x)}La_xTaO_{(3+x)}$ has been investigated. To the best of our knowledge, this is the first report covering sensitization of $NaTaO_3$ by metallo porphyrins to enable visible light utilization.

2. Experimental

2.1. Preparation of catalysts

5, 10, 15, 20-Tetra phenyl porphinato Cobalt(II) (CoTPP) was synthesised using reported procedures [34,35]. $NaTaO_3$ and 2.0% (w/w) lanthanum promoted $NaTaO_3$ catalysts were prepared by hydrothermal route [36,37]. 0.6 g of NaOH dissolved in 20 ml of water (0.75 M) and 0.442 g of Ta_2O_5 were added into a teflon lined stainless steel autoclave. After hydrothermal treatment at 140 °C for 12 h, the precipitate was collected, washed with deionized water and ethanol and finally several times with water and dried at 80 °C for 5 h. La modified $NaTaO_3$, ($Na_{(1-x)}La_xTaO_{(3+x)}$ with x = 0.00014 for 2.0% w/w of La) was prepared by the same procedure, by adding 0.0117 g of La_2O_3 along with NaOH and Ta_2O_5 for hydrothermal treatment. 1.0% w/w −CoTPP/$Na_{(1-x)}La_xTaO_{(3+x)}$ composite was prepared by adopting the method reported previously [38]. Briefly, 10 mg of CoTPP was dissolved in 20 ml of ethanol, followed by 1 g of $Na_{(1-x)}La_xTaO_{(3+x)}$ support with stirring. The resulting solution was refluxed at 80 °C for 130 min. The solvent was removed by evaporation under vacuum and the solid sample was dried at 60 °C for 6 h to obtain. 1.0% w/w −CoTPP/$Na_{(1-x)}La_xTaO_{(3+x)}$ (Actual CoTPP loading-0.99% w/w)

2.2. Computational details

All the calculations in the present study were carried out using Gaussian 09 program package [39]. In order to calculate the reduction potential of the CoTPP complex, density functional theory (DFT) was used. The geometry optimization of the complex was performed at Becke's three-parameter exchange Lee, Yang and Parr correlation (B3LYP) hybrid functional with lanl2dz basis set [40]. The vibrational frequency analysis of the optimized geometry confirmed that the optimized geometry corresponded to minimum on the potential energy surface as revealed from the real values for all vibrational frequencies. Time-dependent density functional theory (TDDFT) calculations were carried out to simulate the electronic transitions at the same basis set. The optimized geometry of the CoTPP is shown in Fig. 1.

2.3. Characterization of catalysts

Phase analyses of the catalysts was carried out by X-ray diffractometer (Rigaku-MiniFlex-II) using Cu Kα radiation (λ=1.54056 Å) with the scan range of 2θ = 5–90° at a speed of 3°/min. The crystallite sizes were calculated by the Scherrer's formula, $t = K\lambda/\beta \cos\theta$, where t is the crystallite size, K is the constant dependent on crystallite shape (0.9 for this case) and λ = 1.54056 Å, β is the FWHM (full width at half maximum) and θ is the Bragg's angle.

Diffuse reflectance spectra of the catalysts in the UV–vis region were recorded using a Thermo Scientific Evolution 600 spectrophotometer equipped with a Praying Mantis diffuse reflectance accessory.

Fourier Transform Infrared Spectra were collected at room temperature by using Perkin-Elmer FTIR spectrophotometer in the range 4000–400 cm^{-1}.

Photoluminescence spectra were recorded under the excitation with a 450W Xenon lamp and the spectra were collected using JobinYvon Fluorolog-3-11 spectro fluorimeter.

Surface area and pore volume of the catalysts were determined using Micromeritics ASAP 2020. Samples were degassed at 373 K for 2 h and at 423 K for 3 h. Pure nitrogen at liquid nitrogen temperature (77 K) was used.

Transmission electron micrographs were recorded using JEOL 3010 model. Few milligrams of the samples (1–2 mg) were dispersed in few mL (1–2 ml) of ethanol by ultra-sonication for 15 min. A drop of the dispersion was placed on a carbon coated copper grid and allowed to dry in air at room temperature.

Scanning electron micrographs were recorded using FEI, Quanta 200, equipped with EDXA attachment for elemental analysis. The samples in the powder form were taken on the carbon tape and mounted on the SEM sample holder.

2.4. Photo catalytic reduction of CO_2

Activity of the catalysts in UV visible region (300–700 nm) was evaluated in batch mode, using jacketed, all glass reactor (620 ml) [41] fitted with quartz window (5 cm dia) and filled with 400 ml of aqueous 0.2 N NaOH solution. Besides increasing the solubility of CO_2, alkaline water acts as hole scavenger. 0.4 g of catalyst was dispersed in the alkaline solution with vigorous stirring (400 rpm). Increasing the stirring rate beyond 400 rpm did not increase the conversion, indicating that under the present experimental conditions, the mass transfer limitations are overcome at this speed. Aqueous alkaline solution (pH-13.0) was saturated with CO_2 by continuous bubbling for 30 min after which pH reduced to 8.0. Reactor in-let and out-let valves were then closed and irradiation with Hg lamp with 77W power (from WACOM HX-500 lamp house) was started. Gas and liquid phase samples were taken out at periodic intervals with gas-tight/liquid syringes and analysed by GC. Liq-

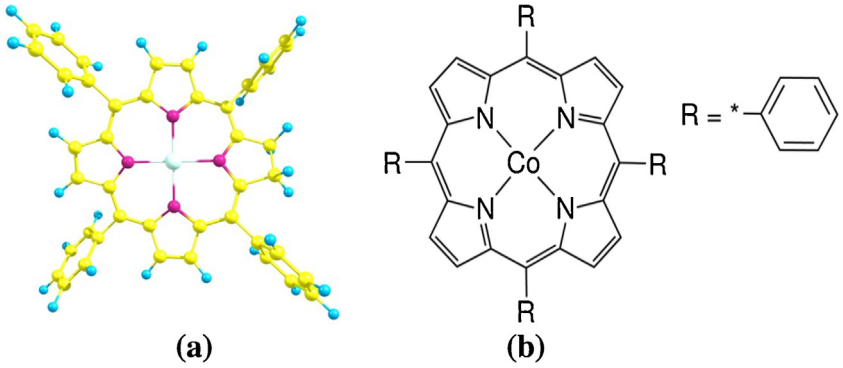

Fig. 1. meso-Tetra phenyl porphyrin cobalt(II) complex (a) Optimized geometry [- Cobalt, - Nitrogen, - Carbon, - Hydrogen] (b) Structure.

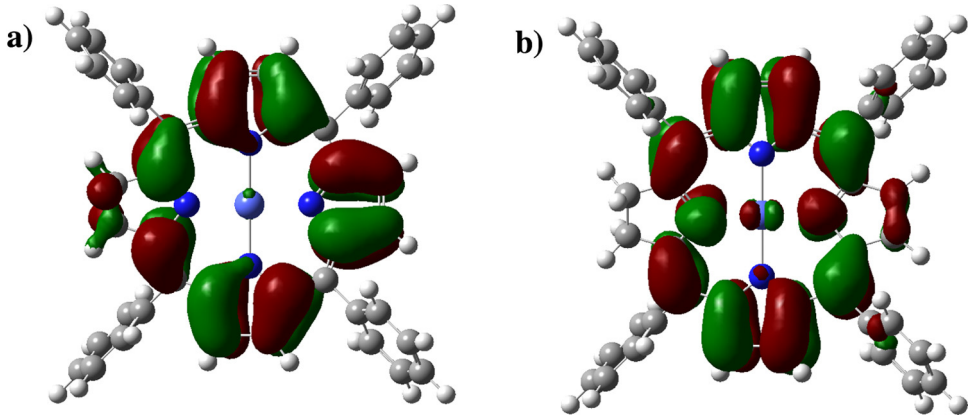

Fig. 2. Schematic representation of (a) HOMO and (b) LUMO orbitals of the Cobalt tetra phenyl porphyrin Complex.

uid phase products (hydrocarbons) were analysed on PoraPlot Q capillary column with FID and gas phase products on Molecular Sieve 13X column with TCD. Potassium ferric oxalate was used as standard for actinometry. Apparent quantum yield (AQY) was calculated based on the quantities of different products formed per hour per gram of the catalyst and using the formula.

$$\text{AQY}(\%) = \frac{\text{Number of reacted electrons}}{\text{Number of incident electrons}} \times 100$$

Blank experiments (reaction with irradiation without catalyst and reaction in dark with catalyst) were conducted to ensure that the products formed were only due to photo reduction of CO_2. When the solution with dispersed catalyst was purged, saturated with nitrogen and irradiated, very small quantities of hydrocarbons, possibly due to the conversion of residual carbon on catalyst surface, was observed up to 6 h, after which no product could be detected. However, on purging and saturation with CO_2, hydrocarbons in increasing amounts up to 20 h and beyond could be observed, thus establishing that the products are actually due to photo catalytic reduction of CO_2. Based on these observations, with each catalyst composite, the solution saturated with nitrogen was first irradiated for 12 h to remove hydrocarbons formed from carbon residues and then saturated with CO_2 so that photo catalytic reduction of CO_2 on clean catalyst could be followed further for 20 h.

3. Results and discussions

Theoretical calculations were employed to get exact positions of HOMO and LUMO levels for CoTPP and compare with $Na_{(1-x)}La_xTaO_{(3+x)}$ band edges. GaussSum program was used to calculate the frontier molecular orbitals (FMOs). HOMO and LUMO orbitals of CoTPP are given in Fig. 2 and molecular orbital diagram for CoTPP is shown in Fig. S1. The calculated molecular orbital energy values are given in Table S1 and the calculated redox potentials of ground (S_0) and excited state (singlet (S_1) of CoTPP complex are given in Table S2. The above calculation shows that HOMO level for the CoTPP complex is at −4.99 V vs absolute vacuum scale (AVS) and that of LUMO is at −2.37 V (vs AVS). Calculated HOMO & LUMO values are closer to those reported in literature [42]. CoTPP is a suitable complex for sensitizing $Na_{(1-x)}La_xTaO_{(3+x)}$, since CoTPP redox potential/conduction band (at −2.07 V vs NHE) is more negative compared to that of $Na_{(1-x)}La_xTaO_{(3+x)}$, with conduction band potential at −1.26 V vs NHE [8,11].

Fig. 3 shows XRD patterns for $NaTaO_3$ (3a), $Na_{(1-x)}La_xTaO_{(3+x)}$ (3b) and CoTPP/$Na_{(1-x)}$ La_x $TaO_{(3+x)}$ (3c). Peaks at 2θ values of 22.9(020), 32.5(200), 40.1(022), 46.6(202), 52.4(301), 58.2(123) for all the three samples indicate that the orthorhombic crystal structure (JCPDS Card No. 25-0863) of the parent phase, $NaTaO_3$, is retained on modifications with La and CoTPP. Sensitized composite shows that there is no significant change in crystal structure as well as crystalline nature of the catalyst since CoTPP is deposited on tantalate surface. However, on substitution of Na^+ ion with La^{3+} in the lattice, a slight shift in the d-line is observed (Fig. S2). Crystallite sizes, calculated by adopting Scherrer's formula, are given in Table 1.

DRS spectra in UV visible region (Fig. 4) shows that the characteristic absorption maximum for $Na_{(1-x)}La_xTaO_{(3+x)}$ located at 302 nm is shifted towards red region, at 330 nm, on sensitization with CoTPP, indicating an interaction between CoTPP and $Na_{(1-x)}La_xTaO_{(3+x)}$. Corresponding band gap values are given in Table 1. Absorption bands for CoTPP (inset), observed at around 419 nm, 541 nm, and 656 nm, are close to those reported for CoTPP [43]. The band at 419 nm corresponds to HOMO-3 → LUMO (81%

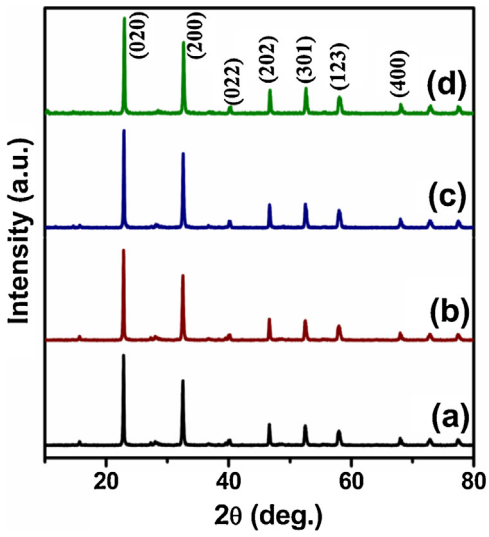

Fig. 3. XRD pattern for neat and sensitized catalyst (a) $NaTaO_3$ (b) $Na_{(1-x)}La_xTaO_{(3+x)}$ (c) $CoTPP/Na_{(1-x)}La_xTaO_{(3+x)}$ (d) Used $CoTPP/Na_{(1-x)}La_xTaO_{(3+x)}$.

Table 1
Crystallite size and band gap energy data for neat and sensitized $Na_{(1-x)}La_xTaO_{(3+x)}$ catalysts.

Photo catalysts	Lattice Parameters (Å)			Crystalline size (nm)	Band gap (eV)
	a	b	c		
$Na_{(1-x)}$ $La_xTaO_{(3+x)}$	5.51	7.78	5.5	47.2	4.1
$CoTPP/Na_{(1-x)}La_xTaO_{(3+x)}$	5.49	7.75	5.5	48.5	3.76

absorption) and band at 541 nm corresponds HOMO → LUMO transition (83% absorption) of a CoTPP complex, both in the visible region. This observation implies that the structure of porphyrin not changed after being loaded on $Na_{(1-x)}La_xTaO_{(3+x)}$ surface.

Presence of CoTPP structure on the surface of sodium tantalate is confirmed by FT-IR spectra shown in Fig. 5. Fig. 5a and b present IR spectra for the neat $Na_{(1-x)}La_xTaO_{(3+x)}$ and $Na_{(1-x)}La_xTaO_{(3+x)}$ sensitized with CoTPP respectively. In Fig. 5b, the band

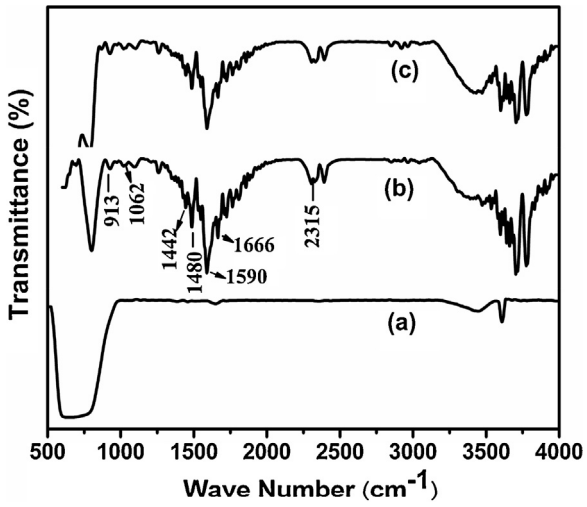

Fig. 5. FT IR spectra for neat and sensitized catalyst (a) $Na_{(1-x)}La_xTaO_{(3+x)}$ (b) $CoTPP/Na_{(1-x)}La_xTaO_{(3+x)}$. (c) Used $CoTPP/Na_{(1-x)}La_xTaO_{(3+x)}$.

at 913 cm^{-1} corresponds to metal-ligand (Co—N) vibration. The bands at 1442 cm^{-1}, 1480 cm^{-1} are assigned to the C—C, C—N stretching vibrations respectively. The above mentioned peaks are the characteristic absorption maxima for metal (Cu, Zn, Co)-TPP complexes [43–45]. Zheng et al. [46] observed similar absorption maxima for CoTPP complex supported on reduced graphene oxide surface. However, two major band shifts in the spectra for $CoTPP/Na_{(1-x)}La_x$ $TaO_{(3+x)}$ vis-à-vis neat CoTPP [45] are observed. The band at 1600 cm^{-1} attributed to the C=C vibration of phenyl ring in neat CoTPP, appears at 1666 cm^{-1} for the $CoTPP/Na_{(1-x)}La_x$ $TaO_{(3+x)}$ and the band at 1000 cm^{-1} due to porphyrin ring vibration in neat CoTPP is now shifted to 1062 cm^{-1} for the composite. These band shifts indicate the interactions between CoTPP and $Na_{(1-x)}La_xTaO_{(3+x)}$. Sensitized tantalate used for 20 h for PCRC reaction also displays similar bands in IR spectrum (Fig. 5c) with respect to fresh material, confirming that no structural changes have taken place during the CO_2 photo reduction process.

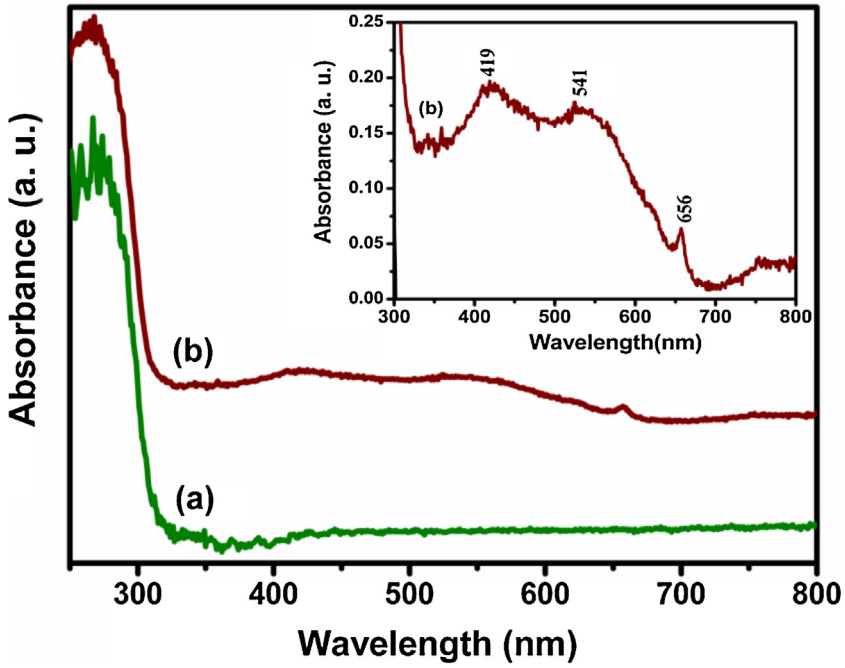

Fig. 4. Diffuse Reflectance spectra for neat and sensitized catalyst (a) $Na_{(1-x)}La_xTaO_{(3+x)}$ (b) $CoTPP/Na_{(1-x)}La_xTaO_{(3+x)}$.

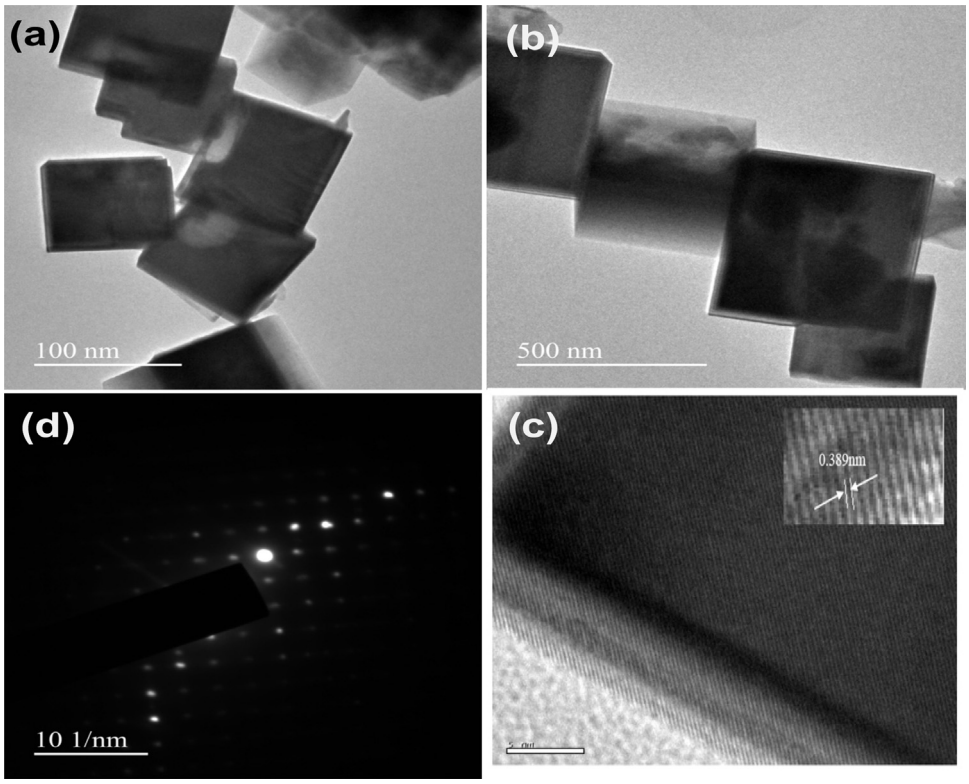

Fig. 6. Electron Microscopic images of TEM image for (a) $Na_{(1-x)}La_xTaO_{(3+x)}$ (b) CoTPP/$Na_{(1-x)}La_xTaO_{(3+x)}$ (c) SAED for CoTPP/$Na_{(1-x)}La_xTaO_{(3+x)}$ (d) HRTEM for CoTPP/$Na_{(1-x)}La_xTaO_{(3+x)}$.

Fig. S3a shows that SEM image of synthesised $Na_{(1-x)}La_xTaO_{(3+x)}$, which is characterized by nano cube morphology. Sensitized tantalate (Fig. S3b) did not show any change in the morphology, which may be due to very small quantity of CoTPP (1% w/w) present on the surface.

TEM (Fig. 6a) further confirms the cubic architecture of the $Na_{(1-x)}La_xTaO_{(3+x)}$ and no changes are observed with sensitized material (Fig. 6b). SAED (Fig. 6c) shows the highly crystalline nature of CoTPP/$Na_{(1-x)}La_xTaO_{(3+x)}$ nano cubes and d-value of 0.389 nm measured from HRTEM (Fig. 6d) corresponds to (002) planes of orthorhombic phase of $Na_{(1-x)}La_xTaO_{(3+x)}$.

STEM-EDS elemental mapping of Na(Kα), Ta(Lα), La(Lα), Co(Kα), O(Kα), N(Kα) shown in Fig. S4 and EDAX data presented in Fig. S5 further confirm the presence of CoTPP complex on the $Na_{(1-x)}La_xTaO_{(3+x)}$ matrix.

Photoluminescence spectra for the neat and sensitized tantalates are presented in Fig. 7. Intensity of the photo luminescence lines for sensitized tantalate is less when compared with those for pristine material, indicating an increase in life time of charge carriers.

PCRC on neat and CoTPP sensitized catalysts were carried out up to 20 h of irradiation. The trends in the formation of different products with irradiation time are plotted in Fig. 8. Yields of all the products formed from CO_2 photo-reduction increase with irradiation time. As shown in Fig. S6 large amounts of methanol is formed when the aqueous alkaline solution is saturated with carbon dioxide, compared to very small quantities formed from the solution saturated with nitrogen, indicating that the observed products are obtained from CO_2 photo reduction and not from carbon impurities on the catalyst surface. Various products observed in the reduction process were identified, quantified and tabulated in Table 2. Based on the initial formation of products from 0 to 10 h, the rate of formation of products and photons consumed for each case, Apparent

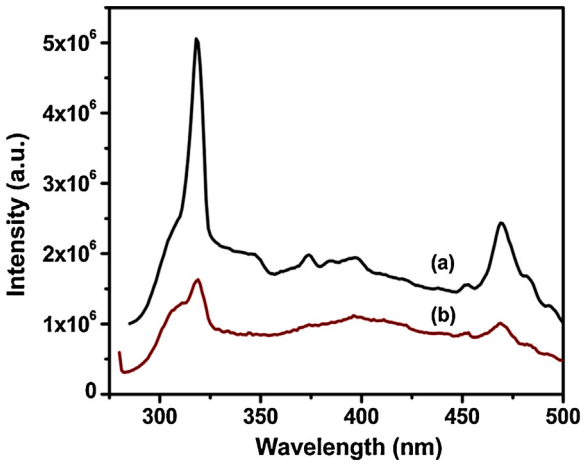

Fig. 7. Photoluminescence Spectra (a) $Na_{(1-x)}La_xTaO_{(3+x)}$, (b) CoTPP/$Na_{(1-x)}La_xTaO_{(3+x)}$.

Quantum Yield (AQY) for both catalysts are calculated and given in Table 2.

Photo catalytic activity data clearly show that, the CoTPP sensitized composite has higher activity, compared with neat $Na_{(1-x)}La_xTaO_{(3+x)}$ (Fig. 9) under similar experimental conditions. After 20 h of illumination, yield of methanol is almost same before and after sensitization of $Na_{(1-x)}La_xTaO_{(3+x)}$, by CoTPP. The rate of formation of 12 e-reduction product, ethanol yield increases in the case of sensitized material. After 20 h of illumination the cumulative ethanol yield was found to be 350 μmol g^{-1}, where as it was only 48 μmol g^{-1} in the case of pristine $Na_{(1-x)}La_xTaO_{(3+x)}$.

CoTPP reduction potential for S_0 (HOMO) and S_1 (LUMO) states are +0.55, −2.00 V vs NHE respectively. As shown in Fig. 10, the excited energy (S_1) of CoTPP is more negative compared to con-

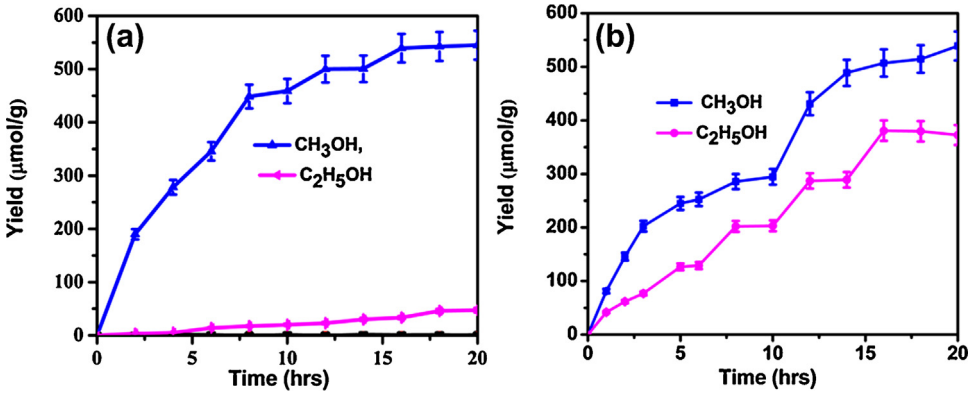

Fig. 8. Trends in photo catalytic activity for CO_2 reduction with alkaline water – Time on stream plots – (a) $Na_{(1-x)}La_xTaO_{(3+x)}$, (b) CoTPP/$Na_{(1-x)}La_xTaO_{(3+x)}$.

Table 2
Products distribution and quantum yield data for neat and sensitized $Na_{(1-x)}La_xTaO_{(3+x)}$ catalysts.

Photo catalysts	Products obtained from CO_2 reduction (µmol$g^{-1}h^{-1}$)								AQY
	CH_4	C_2H_4	C_2H_6	CH_3OH	C_2H_4O	C_2H_5OH	C_3H_6	H_2	(%) * 10^{-3}
$Na_{(1-x)}La_xTaO_{(3+x)}$	0.02	–	–	35.0	4.01	3.1	0.05	0.4	4.0
CoTPP/$Na_{(1-x)}La_xTaO_{(3+x)}$	0.64	0.14	0.07	36.2	3.3	21.4	0.1	0.1	11.5

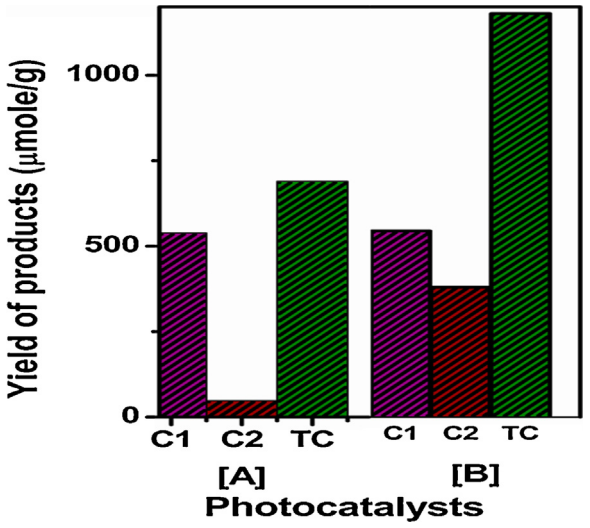

Fig. 9. Comparison of photo catalytic activity for neat and sensitized catalysts: $Na_{(1-x)}La_xTaO_{(3+x)}$, (B) CoTPP/$Na_{(1-x)}La_xTaO_{(3+x)}$. [C1-Methanol, C2-Ethanol, TC-Total Carbon product].

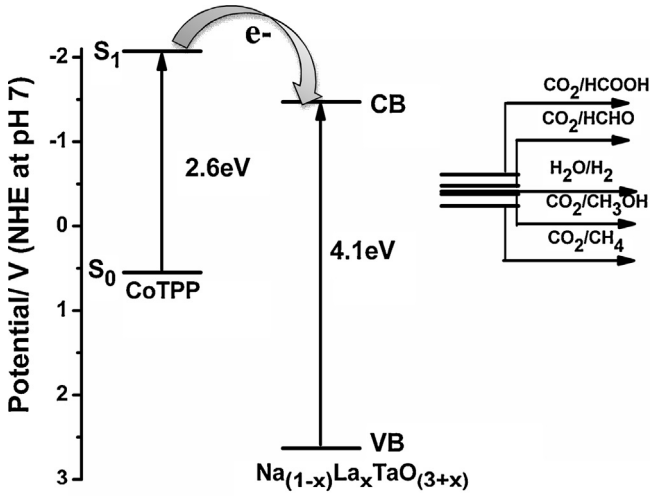

Fig. 10. VB & CB energy levels of CoTPP and $Na_{(1-x)}La_xTaO_{(3+x)}$ vis-a-vis potential for the reduction of CO_2 and oxidation of water.

duction band level of $Na_{(1-x)}La_xTaO_{(3+x)}$. On irradiation of the sensitized catalyst, both CoTPP and $Na_{(1-x)}La_xTaO_{(3+x)}$ absorb light as shown in Scheme 1 below:

$Na_{(1-x)}La_xTaO_{(3+x)}$ VB electrons are excited into CB due to absorption of UV light. Simultaneously, CoTPP molecules get excited and S_0 to S_1 transition occurs due to visible light absorption as shown in Scheme 2. Excited electrons from CoTPP (S_1) are then injected into the CB of La modified sodium tantalate due to thermodynamically favorable position. Thus on sensitization, due to the co-operative effect of both excitations, more excited electrons are available on the CB of active $Na_{(1-x)}La_xTaO_{(3+x)}$ surface, where the adsorbed CO_2 molecules get reduced, forming multi-electron reduction products like ethanol. Thermodynamically, redox potential for the formation of ethanol (−0.33 V vs NHE pH 7) is favorable compared to that of methanol (redox potential −0.38 V vs NHE pH 7).

$$CoTPP + h\upsilon_{(visible)} \longrightarrow CoTPP^*$$

$$Co^{(II)}TPP^* \longrightarrow Co^{(III)}TPP + e^-_{CB/\,(NTO)}$$

$$H_2O + h\upsilon \longrightarrow H^+ + OH^-$$

$$Co^{(III)}TPP + OH^- \longrightarrow Co^{(II)}TPP + OH^{\cdot}$$

$$NaTaO_3 + h\upsilon_{(UV)} \longrightarrow h^+_{VB/(NTO)} + e^-_{CB/\,(NTO)}{}^{\ddagger}$$

$$CO_2 + 6e^-_{CB/\,(NTO)} + 6H^+ \longrightarrow CH_3OH + H_2O$$

$$2CO_2 + 12e^-_{CB\,/(NTO)} + 12H^+ \longrightarrow C_2H_5OH + 3H_2O$$

Scheme 1. Photo chemical reactions on CoTPP/$Na_{(1-x)}La_x$ $TaO_{(3+x)}$ surface. ‡ (NTO – $Na_{(1-x)}La_xTaO_{(3+x)}$).

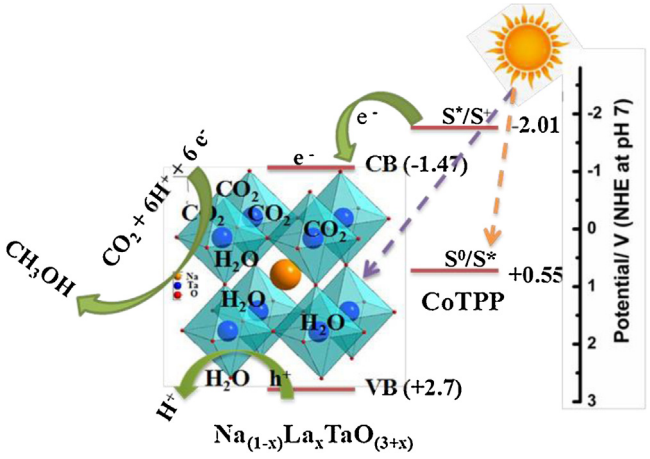

Scheme 2. Photo catalytic reduction of CO_2 on CoTPP sensitized $Na_{(1-x)}La_xTaO_{(3+x)}$.

Absorption of the abundant visible light by CoTPP, appropriate conduction band positions of CoTPP .Vs. the tantalate (to enable electron transfer) and the increase in the life time of the charge carriers are the factors responsible for the observed increase in the formation of multi-electron reduction products like ethanol with the sensitized material compared to pure $Na_{(1-x)}La_xTaO_{(3+x)}$. XRD (Fig. 3d) and FT-IR spectroscopic data (Fig. 5c) for the used sensitized catalyst indicate structural and compositional stability during the reaction.

Li et al. [47] have studied PCRC on $KTaO_3$ nano flakes surface using pure water as reductant, with UV light irradiation and observed only CO and H_2 as major products with traces of methane. This is in contrast to our studies, wherein, aqueous alkaline solution at pH-8.0 as the medium and UV–vis range radiation, are employed. At pH-8.0, bicarbonate (HCO_3^-), species in the alkaline medium act as the active species, undergoing facile photo reduction beyond CO to yield different hydrocarbon products as reported earlier [11], while CO is the major product observed by Li et al. Besides, the conduction band bottom energy level for $Na_{(1-x)}La_xTaO_{(3+x)}$ more negative, at −1.26 V, compared to 0.7 V (both Vs NHE at pH = 0) for $KTaO_3$, which signifies higher reduction capability for $Na_{(1-x)}La_xTaO_{(3+x)}$.

To the best of our knowledge there is no report on the sensitization of $NaTaO_3$ by visible light harvesting compounds like phthalocyanins or porphyrins, especially for PCRC. However, sensitization of TiO_2 by metallo (Co, Cu, Zn) phthalocyanins for PCRC has been studied, with formic acid, formaldehyde and methanol as major products [48–50]. Li et al. [51] have observed CO & CH_4 as products of PCRC on asymmetric Zn porphyrin sensitized TiO_2 and proposed Total Electron Consumed Number (TECN) as the parameter to express overall photo catalytic activity. Table S3 presents the TECN values for similar sensitizer-photo catalyst composites for PCRC. TECN values obtained in the present investigation are in line with those reported for similar systems. Porphyrin moieties are highly effective as sensitizers for photo catalysts like sodium tantalate.

4. Conclusions

Lanthanum modified sodium tantalate, $Na_{(1-x)}La_xTaO_{(3+x)}$, in conjunction with cobalt (II) tetra phenyl porphyrin (CoTPP) as sensitizer, displays significant activity for the photo catalytic reduction of CO_2 with water. Methanol and ethanol are the major products, besides trace levels of methane, ethane and ethylene. HOMO and LUMO energy level characteristics and redox potentials show that sensitization of $Na_{(1-x)}La_xTaO_{(3+x)}$, with visible light is favoured. Sensitized tantalate composite simultaneously absorbs both visible and UV radiation, resulting in the direct transfer of photo generated electrons to its conduction band. Sensitization also retards charge carrier recombination rates, as indicated by the photo luminescence spectral data for the pristine and sensitized $Na_{(1-x)}La_xTaO_{(3+x)}$. These factors contribute towards enhancement of photo catalytic activity that enables multi-electron reduction process leading, to an increase in the formation of ethanol. Sensitized catalyst exhibits chemical and structural stability after 20 h of irradiation.

Acknowledgements

Authors are thankful to DST, Government of India, for establishing the research facilities at NCCR and IIT Madras for infrastructure support. VJ expresses her gratefulness to M/s Hindustan Petroleum Corporation Ltd., Mumbai for the award of a Research Associate ship.

Appendix A. Supplementary data

Supplementary data associated with this article can be found, in the online version, at http://dx.doi.org/10.1016/j.molcata.2016.04.027.

References

[1] Y. Izumi, Coord. Chem. Rev. 257 (2013) 171.
[2] V. Jeyalakshmi, K. Rajalakshmi, R. Mahalakshmy, K.R. Krishnamurthy, B. Viswanathan, Res. Chem. Intermed. 39 (2013) 2565.
[3] V. Jeyalakshmi, R. Mahalakshmy, K.R. Krishnamurthy, B. Viswanathan, Mater. Sci. Forum 734 (2013) 1.
[4] S. Das, W.M.A. Wan Daud, RSC Adv. 4 (2014) 20856.
[5] P. Zhang, J. Zhang, J. Gong, Chem. Soc. Rev. 43 (2014) 4395.
[6] P. Kanhere, Z. Chen, Molecules 19 (2014) 19995–20022.
[7] C.C. Hu, H. Teng, Appl. Catal. A: Gen. 331 (2007) 44.
[8] H. Kato, K. Asakura, A. Kudo, J. Amer. Chem. Soc. 125 (2003) 3082.
[9] H. Kato, A. Kudo, J. Phys. Chem. B 105 (2001) 4285.
[10] K. Teramura, S. Okuokab, H. Tsuneoka, T. Shishido, T. Tanaka, Appl. Catal. B 96 (2010) 565.
[11] V. Jeyalakshmi, R. Mahalakshmy, K.R. Krishnamurthy, B. Viswanathan, Cat. Today 266 (2016) 160–167.
[12] M. Li, P. Li, K. Chang, T. Wang, L. Liu, Q. Kang, S. Ouyang, J. Ye, Chem. Comm. 51 (2015) 7645.
[13] P. Kanhere, P. Shenai, S. Chakraborty, R. Ahuja, J. Zhenge, Z. Chen, Phys. Chem. Chem. Phys. 16 (2014) 16085.
[14] P.D. Kanhere, J. Zheng, Z. Chen, J. Phys. Chem. C 115 (2011) 11846.
[15] P. Kanhere, J. Zheng, Z. Chen, Int. J. Hydrog. Energy 37 (2012) 4889.
[16] X. Zhou, J. Shi, C. Li, J. Phys. Chem. C 115 (2011) 8305–8311.
[17] L. An, H. Onishi, ACS Catal. 5 (2015) 3196.
[18] Y. Liu, Y. Su, H. Han, X. Wang, J. Nanosci. Nanotech. 13 (2013) 853.
[19] P. Han, X. Wang, Y.H. Zhao, C. Tang, Adv. Mater. Res. 79–82 (2009) 1245.
[20] L. Qi, X. Li, J. Sol-Gel Sci. Technol. 69 (2014) 625.
[21] H. Fu, S. Zhang, L. Zhang, Y. Zhu, Mater. Res. Bull. 43 (2008) 864–872.
[22] D.-R. Liu, C.-D. Wei, B. Xue, X.-G. Zhang, Y.-S. Jiang, J. Hazardous Mater. 182 (2010) 50–54.
[23] Z.G. Yi, J.H. Ye, J. App. Phys 106 (2009) 074910.
[24] M. Yang, X. Huang, S. Yan, Z. Li, T. Yu, Z. Zou, Mater. Chem. Phys 121 (2010) 506.
[25] Z.G. Yi, J.H. Ye, Phys. Lett. 91 (2007) 254108.
[26] P. Kanhere, J. Nisar, Y. Tang, B. Pathak, R. Ahuja, J. Zheng, Z. Chen, J. Phys. Chem. C 116 (2012) 22767.
[27] A. Iwase, K. Saito, A. Kudo, Bull. Chem. Soc. Jpn. 82 (2009) 514.
[28] S. Sato, T. Morikawa, S. Saeki, T. Kajino, T. Motohiro, Angew. Chem. Int. Ed. 49 (2010) 5101.
[29] K. Yamanaka, S. Sato, M. Iwaki, T. Kajino, T. Morikawa, J. Phys. Chem. C 115 (2011) 18348.
[30] L. Giribabu, R. Kanaparthi, Curr. Sci. 104 (2013) 847–855.
[31] D. Christopher, M.V. Windle, A.K. Campian, D. Klair, A. Elizabeth, R.N. Robin, J. Schneider, Chem. Commun. 48 (2012) 8189.
[32] G. Yao, J. Li, Y. Luo, W. Sun, J. Mol. Cat. A: Chem. 361 (2012) 29.
[33] W.M. Campbell, A.K. Burrell, D.L. Officer, K.W. Jolley, Coord. Chem. Rev. 248 (2004) 1363.
[34] J.S. Lindsey, R.W. Wagner, J. Org. Chem. 54 (1989) 828.
[35] A. Adler, F.R. Longo, F. Kampas, J. Kim, J. Inorg. Nucl. Chem. 32 (1970) 2443.
[36] X. Li, J. Zang, J. Phy. Chem. C 113 (2009) 19411.
[37] J.W. Liu, G. Chen, Z.H. Lia, Z.G. Zhang, Int. J. Hydrogen Energy 32 (2007) 2269.

[38] J. Niu, B. Yao, Y. Chen, C. Peng, X. Yu, J. Zhang, G. Bai, App. Surface Sci. 271 (2013) 39.
[39] M.J. Frisch, Gaussian 09, Revision B.01; Gaussian, Inc.: Wallingford, CT, 2010.
[40] R. Kumar, M. Sankar, Inorg. Chem 53 (2014) 12706.
[41] K. Rajalakshmi, V. Jeyalakshmi, K.R. Krishnamurthy, B. Viswanathan, Ind. J. Chem. 51A (2012) 411.
[42] M.-S. Liao, S. Scheiner, J. Chem. Phys. 117 (2002) 205.
[43] G. Yao, J. Li, Y. Luo, W. Sun, J. Mol. Catalysis A Chem. 361 (2012) 29.
[44] Q. Wang, W.M. Campbell, E.E. Bonfantani, K.W. Jolley, D.L. Officer, P.J. Walsh, K. Gordon, R. Humphry-Baker, M.K. Nazeeruddin, M. Gra1tzel, J. Phys. Chem. B 109 (2005) 15397.
[45] A.V. Salker, S.D. Gokakakar, Intern. J. Phys. Sci. 4 (2009) 377.
[46] L. Zheng, D. Ye, L. Xiong, J. Xu, K. Tao, Z. Zou, D. Huang, X. Kang, S. Yang, J. Xia, Anal. Chim. Acta 768 (2013) 69.
[47] K. Li, A.D. Handoko, M. Khraisheh, J. Tang, Nanoscale 6 (2014) 9767.
[48] Z. Zhao, J. Fan, M. Xie, Z. Wang, J. Clean. Prod. 17 (2009) 1025.
[49] Z.H. Zhao, J.M. Fan, Z.Z. Wang, J. Clean. Prod. 15 (2007) 1894.
[50] G. Mele, C. Annese, L. D'Accolti, A. De Riccardis, C. Fusco, L. Palmisano, G. Vasapllo, Molecules 20 (2015) 396.
[51] K. Li, L. Lin, T. Peng, Y. Guo, R. Li, J. Zhang, Chem. Commun. 51 (2015) 12443.